

Silver nanoparticles: a novel radiation sensitizer for glioma?[†]

Cite this: *Nanoscale*, 2013, 5, 11829

Peidang Liu,^{‡ab} Zhihai Huang,^{‡a} Zhongwen Chen,^a Ruizhi Xu,^a Hao Wu,^a Fengchao Zang,^c Cailian Wang^d and Ning Gu^{*a}

Malignant gliomas are the most common primary intracranial tumors with a dismal prognosis. Previous investigations by our group demonstrated the radiosensitizing effect of silver nanoparticles (AgNPs) on glioma cells *in vitro*. The goal of the present study was to evaluate the efficacy of intratumoral administration of AgNPs in combination with a single dose of ionizing radiation at clinically relevant MV energies for the treatment of C6 glioma-bearing rats. AgNPs (10 or 20 $\mu\text{g}/10 \mu\text{l}$) were stereotactically administered on day 8 after tumor implantation. One day after AgNP injection, rats bearing glioma received 10 Gy radiation. The mean survival times were 100.5 and 98 days, the corresponding percent increase in life spans was 513.2% and 497.7%, and the cure rates were 41.7 and 38.5% at 200 days for the 10 and 20 μg AgNPs and radiation combination groups, respectively. In contrast, the mean survival times for irradiated controls, 10 and 20 μg AgNPs alone, and untreated controls were 24.5, 16.1, 19.4, and 16.4 days, respectively. Furthermore, a cooperative antiproliferative and proapoptotic effect was obtained when gliomas were treated with AgNPs followed by radiotherapy. Our results showed the therapeutic efficacy of AgNPs in combination with radiotherapy without apparent systemic toxicity, suggesting the clinical potential of AgNPs in improving the outcome of malignant glioma radiotherapy.

Received 19th March 2013

Accepted 22nd July 2013

DOI: 10.1039/c3nr01351k

www.rsc.org/nanoscale

Introduction

Malignant gliomas, characterized by relentless invasive growth and a high tendency to recur, are the most common primary intracranial tumors.¹ Conventional treatment usually consists of surgery followed by radiotherapy and/or chemotherapy. However, the diffusely infiltrative nature of these malicious brain tumors makes a complete surgical resection almost impossible. Furthermore, high grade gliomas, particularly glioblastoma multiforme, exhibit high resistance to radiotherapy and chemotherapy.² Despite decades of intensive efforts, clinical outcome is still poor, with a median overall survival of less than 15 months for patients with glioblastomas.³

The emergence of nanotechnology provides new and powerful tools for imaging, diagnosis and treatment of

cancer.^{4–6} Due to their unique characteristics including high surface-to-volume ratio, broad optical properties, and facile surface chemistry, metal nanoparticles, in particular noble metal nanoparticles, may be useful in killing cancer cells synergistically with conventionally used radiotherapy.⁷

Gold nanoparticles (AuNPs) can enhance the biological effective dose of radiation in cell experiments,^{8,9} mice models,^{10,11} and through Monte Carlo calculations.¹² However, in our previous report, AuNPs modified with proteins from fetal bovine serum showed little effect on glioma cell survival across different doses of ionizing radiation at MV energy levels,¹³ which contrasted with the results of previous studies performed with AuNPs coated with PEG or amino acids in mice colorectal adenocarcinoma and breast cancer cells.^{10,14} Hypothetically, the different coatings of the AuNPs used may be responsible for the different outcomes observed. Another possible explanation is that radiosensitization of AuNPs is cell specific.¹⁵

It is worth noting that, of various noble metal nanomaterials, the research on silver nanoparticles (AgNPs) is a particular hotspot owing to their well known excellent surface enhanced Raman scattering^{16–18} and broad-spectrum antimicrobial activities.^{19,20} In our previous study, we proved, for the first time, that AgNPs could function in enhancing radiation-induced killing of glioma cells. Treating the malignant cells with AgNPs led to dose-dependent cytotoxicity, with smaller size particles (20 and 50 nm) being the most cytotoxic at relatively harmless radiation doses.¹³ More recently, the enhanced radiation effects of silver

^aJiangsu Key Laboratory for Biomaterials and Devices, State Key Laboratory of Bioelectronics, School of Biological Science and Medical Engineering, Southeast University, Nanjing 210096, PR China. E-mail: guning@seu.edu.cn; Fax: +86 25 83272476; Tel: +86 25 83272460

^bInstitute of Neurobiology, School of Medicine, Southeast University, Nanjing 210009, PR China

^cJiangsu Key Laboratory of Molecular and functional Imaging, Department of Radiology, School of Medicine, Southeast University, Nanjing 210009, PR China

^dTumor Center of Zhongda Hospital, Southeast University, Nanjing 210009, PR China

[†] Electronic supplementary information (ESI) available. See DOI: 10.1039/c3nr01351k

[‡] P.D. Liu and Z.H. Huang contributed equally to the manuscript.

nanomaterials were confirmed in other cancer cells.^{21,22} Due to the differences of microenvironments and condition control-abilities, however, it is unclear whether our *in vitro* findings also apply *in vivo*.

The aim of the present study was to evaluate the efficacy and safety of intratumoral administration of small size AgNPs in combination with ionizing radiation at clinically relevant MV energies for the treatment of C6 glioma-bearing rats, and to assess some possible mechanisms of radiosensitizing effects of AgNPs. These findings will provide an important theoretical basis for the potential clinical application of AgNPs as a novel radiation sensitizer.

Experimental section

Preparation of AgNPs

AgNPs were synthesized using the improved electrochemical method based on the continuous-flow process as previously described.^{23,24} The synthesis conditions were as follows: the reaction temperature was 60 °C, the electrolytic voltage was 15 V, the solution flow-rate was 80 ml h⁻¹, and the concentration of PVP was 5 mg ml⁻¹. After synthesis of silver colloidal solution, AgNP powders were obtained following filtration, centrifugal concentration and vacuum drying at 60 °C. The morphologies of AgNPs were studied by TEM (JEM-2000EX JEOL) and the size statistical distributions were determined by counting one thousand AgNPs in TEM photographs. The UV-Vis absorption spectrum of AgNPs was measured using a UV-Vis spectrophotometer (Shimadzu UV-3600) from 700 nm to 200 nm. Dynamic light scattering (DLS) and zeta potential measurements were carried out at room temperature using a Zetaplus Analyzer (Zetaplus, Brookhaven, USA).

Cells and rats

Rat C6 glioma cells were obtained from the Chinese Academy of Sciences in Shanghai originally from American Type Culture Collection (Manassas, VA, USA), cultured in Dulbecco's modified Eagle's medium (DMEM, Hyclone) supplemented with 10% fetal bovine serum (FBS, Gibco), penicillin, and streptomycin at 37 °C in an atmosphere of 5% CO₂. Adult male Wistar rats, weighing 230–250 g at the beginning of the experiments, were purchased from National Rodent Laboratory Animal Resources (Shanghai Branch, China). All animals were housed in separate cages, with access to standard laboratory food and water *ad libitum*, and kept in a regulated environment (22–22 °C) under a 12 h : 12 h light/dark cycle starting at 7:00 AM. The use of animals in this study was approved by the Institutional Animal Care and Use Committee of the Southeast University.

Tumor model

C6 glioma cells were detached using trypsin when reaching near 80% confluency of the plate, washed once with DMEM without FBS, and resuspended in DMEM at an amount of 1 × 10⁸ ml⁻¹. Only the second generation of cells after recovery from liquid nitrogen was used in the experiments. Rats were anesthetized by a peritoneal injection with 5 μl g⁻¹ of 7.5% chloral hydrate

and placed in a small-animal stereotactic frame (RWD Life Science, Shenzhen, China). After shaving and disinfection of the skin, a sagittal incision was made to expose the skull, followed by a burr hole 1 mm anterior and 3 mm lateral from the bregma using a small drill. A 25 μl Hamilton syringe containing 10 μl of cell suspension was inserted into the right striatum at a depth of 6 mm from the skull surface. On completion of the injection, the needle was left in place for 5 min and withdrawn slowly. The scalp incision was then closed with surgical sutures, and the animals were returned to their home cages. The glioma-bearing rats were randomly divided into 6 groups: untreated control, 10 μg of AgNPs, 20 μg of AgNPs, irradiated control, 10 μg of AgNPs + 10 Gy, and 20 μg of AgNPs + 10 Gy. Ten microliters of deionized water or AgNPs (10 or 20 μg, diluted in deionized water) were intratumorally administered using a stereotactic technique on day 8 after tumor implantation. The choice of concentration of AgNPs was based on our preliminary study (see Tables S1 and S2 in the ESI†).

Magnetic resonance imaging (MRI)

MRI was used in the rat malignant glioma model for confirmation of the presence or absence of tumor on day 7 or day 200 postinoculation. MRI was undertaken on a 7.0 T animal MRI scanner (70/16 PharmaScan, Bruker Biospin GmbH, Germany) using a 38 mm birdcage rat brain quadrature resonator for radiofrequency transmission and reception as previously described.²⁵ Briefly, rats were anesthetized using inhaled isoflurane/O₂ (3% for induction and 1.5–2% for maintenance). During the MRI scan, the rats were prostrated on a custom-made holder to minimize head motion while respiration was maintained at a rate of 50 breaths min⁻¹. Scout T₂-weighted imaging (T₂WI) in three planes with a fast spin echo pulse sequence was first acquired to control rat head positioning. Next, a coronal T₂WI scan was acquired using a rapid-acquisition relaxation-enhancement pulse sequence with the following parameters: field of view = 3 × 3 cm, matrix size = 256 × 256, repetition time = 2500 ms, echo time = 33 ms, slice thickness = 1.0 mm, slice gap = 1.0 mm, and acquisition time = 1 min 20 s.

Irradiation

Approximately 24 h after AgNP injection, rats were anesthetized by a peritoneal injection with 5 μl g⁻¹ of 7.5% chloral hydrate and immobilized with a fixed apparatus, and the tumor ipsilateral half brain was irradiated with a vertical beam of 6 MV X-rays generated from a linear accelerator (Siemens, Germany) at a dose rate of 200 MU min⁻¹. The delivered dose was 10 Gy per rat. The radiation field was 15 × 15 cm at a source–surface distance of 100 cm.

Histology, immunohistochemistry, and TUNEL assay

Animals from the 6 groups were deeply anesthetized and perfused transcardially with 4% paraformaldehyde in phosphate-buffered saline (PBS) 6 h postradiotherapy.^{26,27} Brains were removed from the skulls and post-fixed overnight at 4 °C in 4% paraformaldehyde. Next day, the brains were transferred to 30% sucrose in PBS solution for 48 h at 4 °C. Coronal sections

with a thickness of 10 μm were cut using a cryostat microtome (Leica CM1900, Germany). Hematoxylin and eosin (H&E) staining was used to visualize the tumor area and tumor necrosis. For evaluating cell proliferation, immunostaining for proliferating cell nuclear antigen (PCNA) was used. Mouse monoclonal antibody against PCNA (Abcam) was diluted 1 : 300 in blocking solution containing 0.3% Triton X-100 and incubated overnight at 4 $^{\circ}\text{C}$. After being washed in PBS, the sections were incubated with a biotinylated secondary antibody for 2 h. They were washed and further incubated with a streptavidin-biotin-peroxidase complex (Vector Laboratories). Apoptotic activity was examined using the terminal deoxynucleotidyl transferase-mediated deoxyuridine triphosphate nick end labeling (TUNEL) method (In Situ Cell Death Detection Kit; Roche Molecular Biochemicals) essentially according to the manufacturer's instructions. Sections were then visualized with 3,3-diaminobenzidine as a chromogen and counterstained with Harris hematoxylin. Negative control sections received identical staining preparations, except that the primary antibody or terminal transferase was omitted. The percentage of proliferation or apoptosis was calculated as the proportion of positive cells to the total number of cell nuclei.

Animal observation

After treatment with AgNPs by injection, the animals were examined daily for any changes in morphology and behavior, and weighed thrice a week. The combination of sustained weight loss, ataxia, and periorbital bleeding has been shown to be indicative of progressively growing tumors.²⁸ Rats too weak to feed and to stand were euthanized with carbon dioxide gas. The time of euthanasia was recorded and used in the survival analysis. The long-term survivors were defined as animals living more than 200 days, and the surviving rats were imaged with MRI and then perfused with 4% paraformaldehyde at this time point. Coronal slices (10 μm thick) were stained with H&E, and examined microscopically to assess histopathological changes.

Statistical analysis

All data were expressed as means \pm SEM. The survival analysis was done using the Kaplan–Meier survival curve and the log-rank test. The percent increased life span was determined relative to the mean survival time (MST), or median survival time (MeST) of untreated controls as $[(\text{MST} - \text{MST}_{\text{Control}})/\text{MST}_{\text{Control}}] \times 100$. Data on cell proliferation and apoptosis were analyzed by one-way ANOVA followed by a Tukey–Kramer post hoc test. Values of $P < 0.05$ were considered statistically significant.

Results and discussion

Characterization of nanoparticles

In order to improve the therapeutic index, in the current study, the smaller size AgNPs were synthesized and used, since our *in vitro* study demonstrated that the radiosensitizing effect of AgNPs was in a size-dependent manner, with smaller size particles being the most effective.¹³ The size distribution and optical absorption of the PVP-coated AgNPs are characterized

by TEM and spectrophotometry and the results are shown in Fig. 1. The average size of AgNPs synthesized in colloidal solution was 10.2 ± 0.08 nm (Fig. 1C); however, after drying at 60 $^{\circ}\text{C}$, the size of AgNP powders grew up to 16.1 ± 0.12 nm (Fig. 1D) owing to the ripening of AgNPs. The AgNP powders are easy to redissolve to a silver colloidal solution by adding deionized water. Before and after drying of the solution, AgNPs were predominantly spherical in morphology and were well monodispersed (Fig. 1A and B). The absorption peak of the UV-Vis spectrum was about 410 nm (Fig. 1E), which belongs to the typical surface plasmon resonance absorption band of AgNPs. The DLS size distribution of AgNPs by number was 21.2 ± 0.31 nm, which was consistent with TEM results, and the DLS size distribution by intensity was 88.6 ± 2.10 nm because of the extension of the PVP molecular chain in water and the effect of the nanoparticle's hydration shell. The polydispersity index was 0.29 ± 0.003 according to DLS results, indicating that the AgNPs synthesized using the method have good monodispersity. The zeta potential of AgNPs was -15.5 ± 0.74 mV, so the AgNPs stabilized with PVP were negative.

Antitumor effects of AgNPs in rats bearing glioma

The C6 rat glioma, an experimental model for studies on glioblastoma multiforme,²⁹ was employed in this study for examining the antitumor effects of AgNPs *in vivo*. The results showed

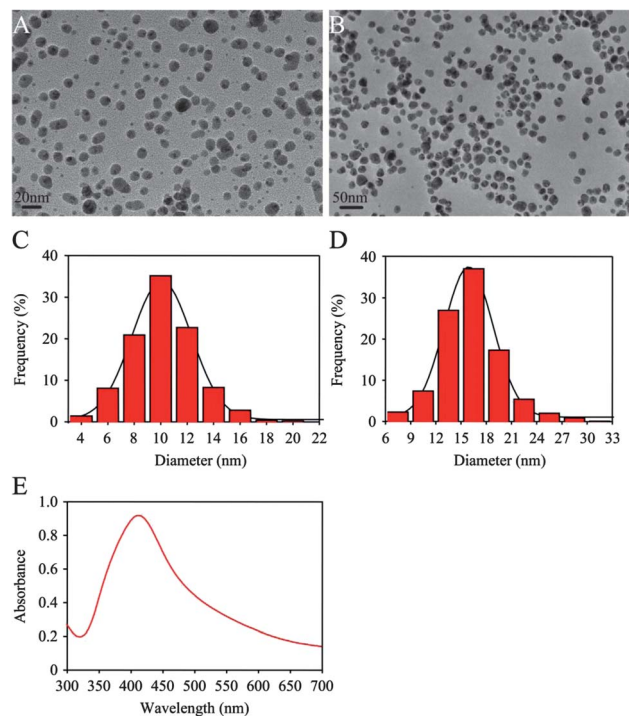


Fig. 1 TEM characterization and the UV-Vis absorption spectrum of silver nanoparticles. Particles were spotted onto carbon-coated Cu grids and dried under air prior to TEM imaging. The particle size distributions were determined by measuring the nanoparticles from micrographs using Image J with $n > 1000$ for each sample. TEM (A) and size distribution (C) of AgNPs before vacuum drying at 60 $^{\circ}\text{C}$. TEM (B) and size distribution (D) of AgNPs after vacuum drying at 60 $^{\circ}\text{C}$. (E) UV-Vis absorption spectrum of AgNPs.

Table 1 Survival times of C6 glioma-bearing rats following intratumoral administration of AgNPs with or without ionizing radiation

Group	No. of rats	Range	Survival times (days)		% Increased life span	
			Mean \pm SEM	Median	Mean	Median
Untreated control	9	14–19	16.4 \pm 0.5	16.5	–2.1	0
10 μ g of AgNPs	10	13–20	16.1 \pm 0.7	16.5	–2.1	0
20 μ g of AgNPs	10	16–26	19.4 \pm 1.1	18.3	18.1	10.6
Irradiated control	10	21–29	24.5 \pm 0.9	24.5	49.5	48.5
10 μ g of AgNPs + 10 Gy	12	25–200 (5) ^a	100.5 \pm 25.4	33.5	513.2	103.0
20 μ g of AgNPs + 10 Gy	13	30–200 (5) ^a	98.0 \pm 23.3	37.0	497.7	124.2

^a The number in parentheses indicates the number of rats surviving >200 days.

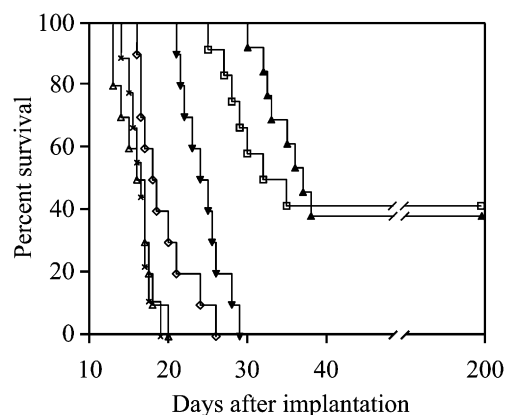


Fig. 2 Kaplan–Meier survival curves for C6 glioma-bearing rats following intratumoral administration of AgNPs with or without ionizing radiation. Survival times in days after tumor implantation have been plotted for untreated animals (x), 10 μ g of AgNPs alone (Δ), 20 μ g of AgNPs alone (\diamond), irradiated control (\blacktriangledown), 10 μ g of AgNPs + 10 Gy (\square), and 20 μ g of AgNPs + 10 Gy (\blacktriangle).

that all tumor-bearing rats in the untreated control group died before day 20 due to an excessive tumor burden (Table 1). No statistically significant difference in MST was found between 10 μ g of AgNP treatment and untreated control groups ($p > 0.05$). However, 20 μ g of AgNP treatment led to a slight but significant enhancement in the life span compared with the untreated controls ($p < 0.05$).

It has been found that AgNPs could inhibit vascular endothelial growth factor (VEGF)-induced angiogenesis in bovine retinal endothelial cells and *in vivo* angiogenesis.^{30,31} Sheikpranbabu *et al.* also demonstrated the inhibitory effect of AgNPs on vascular permeability induced by VEGF, interleukin-1 β , and advanced glycation end products in retinal endothelial cells.^{32,33} Furthermore, AgNP exposure resulted in inhibition of proliferation in human glioblastoma cells.³⁴ The potent antiangiogenic, antivascular permeability and antiproliferative properties of AgNPs indicate that AgNPs may act as a potential antitumor agent. In the present study, 10 μ g of AgNPs alone treatment did not lead to a significant increase in MST, while 20 μ g of AgNPs resulted in a slight but significant enhancement, suggesting that the antitumor activity of AgNPs is dose-dependent. The prolonged survival in animals treated with 20 μ g of AgNPs may be explained by the existence of large necrotic and apoptotic areas close to the nanoparticle deposits. These antitumor

results are consistent with the findings reported by Sriram *et al.*, where the survival time increased in the Dalton's lymphoma ascites mouse model by about 50% in comparison with that of tumor controls, following intraperitoneal injection of AgNPs at a concentration of 500 nM for 15 days.³⁵

Due to their small enough size, when the colloidal particles come into contact with the tumor, uptake of the particles by living cancer cells takes place either positively or passively. In effect, the efficiency of cellular uptake of nanomaterials and the resultant intracellular concentration determine the cytotoxic potential.³⁶ Furthermore, the cellular uptake efficiency is mainly dependent on the nanoparticle concentration.^{37,38} Thus, the therapeutic effects of high dose AgNPs would be due to enhanced internalization and retention of the nanoparticles by glioma cells.

It is well established that different coatings show different toxicity. In this study, we investigated the toxicity of the PVP coating. PVP-coated and naked AgNPs exhibited similar cytotoxicity (see Fig. S1 in the ESI[†]). These data suggested that the toxicity of the AgNPs was attributed to the silver and not the PVP coating.

Therapeutic effects of the combination of AgNPs with radiotherapy

To determine whether the combination of AgNPs and radiotherapy resulted in better antitumor effects in terms of survival than irradiation alone, the radiotherapy was performed following intratumoral administration of AgNPs, and the survival time of the tumor-bearing rats was recorded and analyzed. Survival data are summarized in Table 1 and Kaplan–Meier survival plots are shown in Fig. 2. The irradiated controls had a modest increase in MST to 24.5 days compared with a MST of 16.4 days for the untreated rats. Most importantly, the survival time in the combination therapy groups was significantly enhanced compared with that in the irradiation alone group ($P < 0.001$). Animals that received 10 and 20 μ g of AgNPs combined with radiotherapy had MSTs of 100.5 and 98 days and cure rates of 41.7 and 38.5% at 200 days, respectively. The survival times and cure rates of these two nanoradiotherapy groups were not significantly different from each other ($P > 0.05$).

Based on our non-irradiated data, we evaluated the efficacy of these two doses of AgNPs in conjunction with a single moderate dose of irradiation. Similarly to our *in vitro* findings, we observed that small size AgNPs' administration to

glioma-bearing rats strongly enhanced the biological efficiency of radiation. Glioma-bearing rats that received 10 and 20 μg of AgNPs, followed by 6-MV X-irradiation, had approximately equal mean survival times and cure rates, although 10 μg of AgNPs alone did not show any therapeutic efficacy. Taken together, these results indicate the radiosensitizing effect of AgNPs *in vivo*. In addition, the radiosensitizing effect of 10 μg of AgNPs was not statistically different from 20 μg , suggesting that 10 μg of AgNPs may be the maximally effective dose.

Although the detailed mechanistic effects of radiation on AgNPs that lead to the enhancement of radiosensitivity remain largely unexplored, it is clear that noble metal nanoparticles can act as antennas, providing enhanced radiation targeting with lower radiation doses.⁷ Once activated by high-energy electron beams, these particles create additional short-range secondary electrons.³⁹ The increased production of these low-energy electrons generates large quantities of free radicals, which inflict nonspecific, irreversible damage to the cancer cells that leads to their destruction and multiplies the effects of radiation therapy.

In addition, the accumulation of AgNPs in normal tissues surrounding the tumor was quantitatively assessed by inductively coupled plasma mass spectrometry at different time points. The results showed that the silver concentrations were close to the detection limit of the method (data not shown). Given the low levels of silver, the effect of the nanoparticles on adjacent healthy cells should be negligible.

Antiproliferative and proapoptotic effects of AgNPs combined with radiotherapy

Cell proliferation is an important factor in the prognosis of malignant tumor.^{40,41} Furthermore, apoptosis is considered as a regulator of both intrinsic and extrinsic determinants of the response of tumors to radiotherapy and contributes significantly to the radiosensitivity of tumor cells.⁴² In this study, we examined whether proliferation and apoptosis were associated with the antitumor effects of combination therapy. As shown in Fig. 3, microscopic examination of PCNA-stained tumor sections showed a decrease in PCNA-positive cells after a single dose of radiotherapy as compared with the unirradiated controls. Quantitative analysis revealed that the percentages of proliferation were significantly lower in the AgNPs and radiation combination groups than that in the irradiation alone group ($P < 0.01$). The *in vivo* apoptotic response of glioma cells to AgNPs with or without radiation was investigated by TUNEL staining. Microscopic examination of the tumor sections showed that, compared with the untreated controls, radiotherapy increased the number of TUNEL-positive cells. Importantly, the quantitative evaluation of apoptosis showed that AgNPs in combination with radiotherapy significantly increased the apoptotic index as compared with the irradiated controls ($P < 0.001$). No statistical differences were found between the two nanoradiotherapy groups regarding any of the parameters studied.

The main goal when treating malignancies with radiation therapy is to deprive tumor cells of their reproductive potential.⁴³

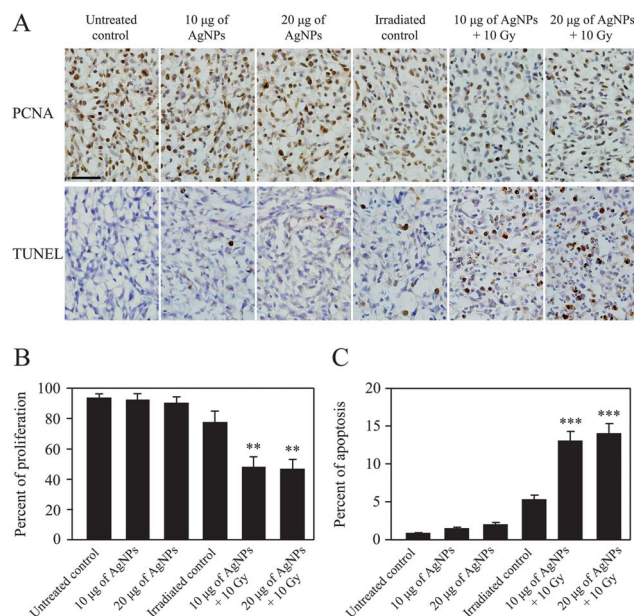


Fig. 3 Reduced proliferation and increased apoptosis caused by AgNPs in combination with ionizing radiation. Rats from each group were sacrificed 6 h postradiotherapy. Ten-micrometer thick cryostat sections were obtained and stained for proliferating cell nuclear antigen (PCNA) or terminal deoxynucleotidyl transferase-mediated deoxyuridine triphosphate nick end labeling (TUNEL), and counterstained with hematoxylin. (A) PCNA and TUNEL staining for each group. Quantitative analyses of proliferation and apoptosis are shown in (B) and (C), respectively. The percentage of proliferation or apoptosis was calculated by averaging the percentages from four different fields in each section. Values are the means \pm SEM of determinations in 5 animals of each group. ** $P < 0.01$, *** $P < 0.001$ compared with irradiated controls. Scale bar: 50 μm .

In the present study, we found that AgNPs, combined with ionizing radiation, had powerful antiproliferative effects on glioma cells in rats. Induction of apoptosis or programmed cell death has been regarded as a promising strategy for the control of the proliferation of cancer cells.⁴⁴ Therefore, we examined the levels of apoptosis *in vivo* at the time of peak apoptosis (*i.e.* 6 h post-irradiation).^{26,27} The apoptotic index significantly increased after combination therapy, but at a lower rate than the observed decrease in the level of proliferating cell nuclear antigen, suggesting that apoptosis may contribute, at least in part, to the antiproliferative effects of AgNPs in conjunction with ionizing radiation.

Table 2 Percentage loss in body weight 3 days and 7 days after AgNP treatment of C6 glioma^a

Group	3 days	7 days
Untreated control	-4.2 ± 0.5	1.2 ± 0.2
10 μg of AgNPs	-2.9 ± 0.3	2.2 ± 0.3
20 μg of AgNPs	-3.1 ± 0.4	0.9 ± 0.2
Irradiated control	1.8 ± 0.2	2.2 ± 0.3
10 μg of AgNPs + 10 Gy	4.5 ± 0.4	4.9 ± 0.7
20 μg of AgNPs + 10 Gy	4.1 ± 0.4	4.6 ± 0.6

^a Values are the means \pm SEM of determinations in 6–13 animals of each group.

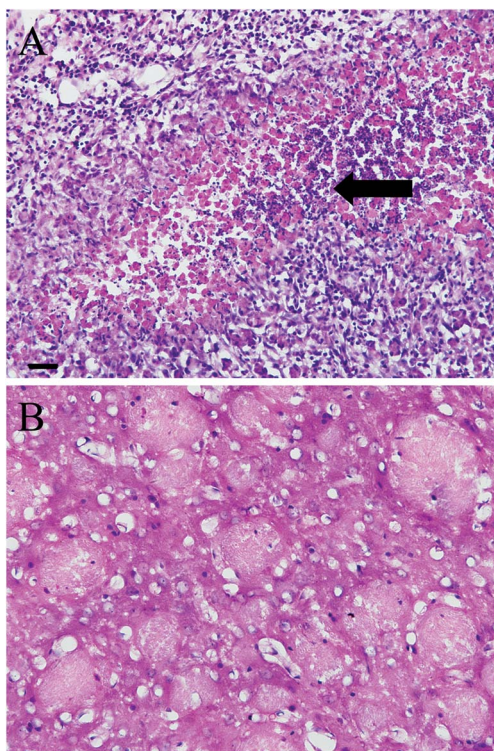


Fig. 4 Histopathological changes of the malignant gliomas. (A) Histology of the C6 glioma in a rat euthanized 1 day after 20 µg of AgNP treatment. Arrow indicates the large necrotic area close to the nanoparticle deposits. (B) Brain of a rat from the combined therapy groups that was alive at the end of the study (200 days), showing numerous fibrotic foci surrounded by gliosis-like margins. Scale bar: 100 µm.

Body weight analysis

Table 2 shows body weight changes of rats receiving different treatments. 3 days after AgNP administration, unirradiated groups exhibited an increase in body weight, and then the body weight decreased due to the effects of brain tumor. However, irradiated groups showed a small loss of body weight (<5%) within the first 7 days after AgNP injection, followed by a gradual regain of weight over time. This body weight loss is attributed primarily to the insult of radiation.

To be clinically useful, a radiosensitizer should significantly increase the therapeutic ratio and should also be non-toxic or minimally toxic.^{45,46} Therefore, the safety of the use of AgNPs was evaluated by determining alteration of body weight and clinical status. Only a small weight loss in the radiation groups was observed within the first 7 days after AgNP injection, indicating AgNPs used, even under radiation conditions, do not cause apparent systemic toxicity.

Histopathologic studies

About 1 day after AgNP injection, large necrotic areas close to the nanoparticle deposits were observed, especially in 20 µg of AgNP treated tumor tissues (Fig. 4A). When animals died, the tumors of the untreated control groups and of the animals given nanotherapy did not differ in histopathology. For rats that

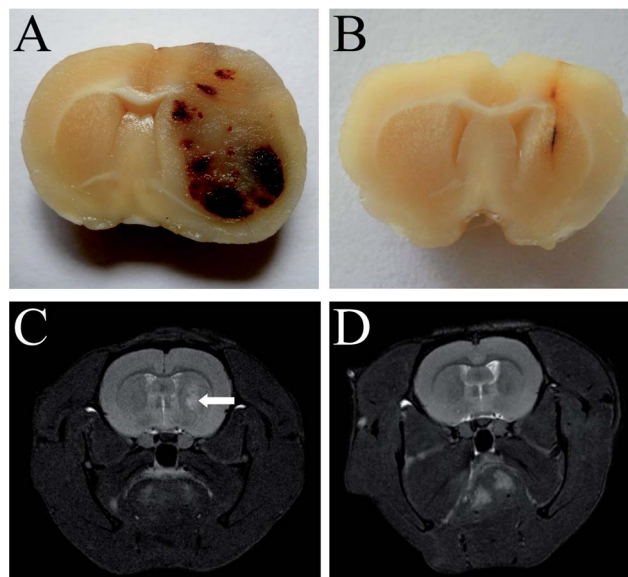


Fig. 5 Frontal slices of brains and T_2 -weighted MR images. Brain slices from an untreated control animal at the end of survival for 200 days (A), or from a glioma-bearing rat surviving for 200 days (B). (C) Image from a representative animal showing well established tumor 7 days after implantation (arrow). (D) Image from a glioma-bearing rat surviving for 200 days showing the absence of tumor.

survived up to 200 days (*i.e.* from the combined therapy groups), the H&E staining results showed numerous fibrotic foci surrounded by gliosis-like margins but no trace of residual tumor (Fig. 4B), which was confirmed by MRI (Fig. 5D), suggesting its irreversible regression.

Conclusions

The purpose of the present study was to evaluate the radiosensitizing effects of PVP-coated AgNPs on the C6 glioma of rats, a well established model for glioblastoma multiforme. The survival time, toxicity, cell proliferation and apoptosis *in vivo* were investigated at two doses. It was found that the combination of AgNPs and radiotherapy resulted in a marked enhancement in the mean survival time, and a near 40% cure rate in glioma-bearing rats without apparent systemic toxicity, which may be due to its potent antiproliferative activity. Further studies are required to clarify the underlying molecular mechanisms. These results suggest the clinical potential of AgNPs in improving the outcome of malignant glioma radiotherapy.

Conflict of interest

No competing financial interests exist.

Abbreviations

AgNPs	Silver nanoparticles
AuNPs	Gold nanoparticles
DMEM	Dulbecco's modified Eagle's medium
DLS	Dynamic light scattering
FBS	Fetal bovine serum

H&E	Hematoxylin and eosin
MeST	Median survival time
MRI	Magnetic resonance imaging
MST	Mean survival time
PBS	Phosphate-buffered saline
PCNA	Proliferating cell nuclear antigen
TUNEL	Terminal deoxynucleotidyl transferase-mediated deoxyuridine triphosphate nick end labeling
T ₂ WI	T ₂ -weighted imaging
VEGF	Vascular endothelial growth factor

Acknowledgements

This work was supported by the National Key Basic Research Program of China (973 Program) (Grant no. 2013CB933904), the National Important Science Research Program of China (Grant no. 2011CB933500), and the National Natural Science Foundation of China (Grant no. 51201034).

References

- 1 L. M. DeAngelis, *N. Engl. J. Med.*, 2001, **344**, 114–123.
- 2 R. Stupp, M. E. Hegi, M. R. Gilbert and A. Chakravarti, *J. Clin. Oncol.*, 2007, **25**, 4127–4136.
- 3 R. Stupp, W. P. Mason, M. J. van den Bent, M. Weller, B. Fisher, M. J. Taphoorn, K. Belanger, A. A. Brandes, C. Marosi, U. Bogdahn, J. Curschmann, R. C. Janzer, S. K. Ludwin, T. Gorlia, A. Allgeier, D. Lacombe, J. G. Cairncross, E. Eisenhauer and R. O. Mirimanoff, *N. Engl. J. Med.*, 2005, **352**, 987–996.
- 4 P. R. Gil and W. J. Parak, *ACS Nano*, 2008, **2**, 2200–2205.
- 5 N. Sanvicens and M. P. Marco, *Trends Biotechnol.*, 2008, **26**, 425–433.
- 6 J. R. Heath and M. E. Davis, *Annu. Rev. Med.*, 2008, **59**, 251–265.
- 7 J. Conde, G. Doria and P. Baptista, *J. Drug Delivery*, 2012, **2012**, 751075.
- 8 F. Geng, K. Song, J. Z. Xing, C. Yuan, S. Yan, Q. Yang, J. Chen and B. Kong, *Nanotechnology*, 2011, **22**, 285101.
- 9 W. Xu, T. Luo, P. Li, C. Zhou, D. Cui, B. Pang, Q. Ren and S. Fu, *Int. J. Nanomed.*, 2012, **7**, 915–924.
- 10 J. F. Hainfeld, D. N. Slatkin and H. M. Smilowitz, *Phys. Med. Biol.*, 2004, **49**, N309–N315.
- 11 X. D. Zhang, D. Wu, X. Shen, J. Chen, Y. M. Sun, P. X. Liu and X. J. Liang, *Biomaterials*, 2012, **33**, 6408–6419.
- 12 S. H. Cho, *Phys. Med. Biol.*, 2005, **50**, N163–N173.
- 13 R. Xu, J. Ma, X. Sun, Z. Chen, X. Jiang, Z. Guo, L. Huang, Y. Li, M. Wang, C. Wang, J. Liu, X. Fan, J. Gu, X. Chen, Y. Zhang and N. Gu, *Cell Res.*, 2009, **19**, 1031–1034.
- 14 T. Kong, J. Zeng, X. Wang, X. Yang, J. Yang, S. McQuarrie, A. McEwan, W. Roa, J. Chen and J. Z. Xing, *Small*, 2008, **4**, 1537–1543.
- 15 S. Jain, J. A. Coulter, A. R. Hounsell, K. T. Butterworth, S. J. McMahon, W. B. Hyland, M. F. Muir, G. R. Dickson, K. M. Prise, F. J. Currell, J. M. O'Sullivan and D. G. Hirst, *Int. J. Radiat. Oncol., Biol., Phys.*, 2011, **79**, 531–539.
- 16 D. He, B. Hu, Q. F. Yao, K. Wang and S. H. Yu, *ACS Nano*, 2009, **3**, 3993–4002.
- 17 Y. Lu, G. L. Liu and L. P. Lee, *Nano Lett.*, 2005, **5**, 5–9.
- 18 D. Yang, S. Chen, P. Huang, X. Wang, W. Jiang, O. Pandoli and D. Cui, *Green Chem.*, 2010, **12**, 2038–2042.
- 19 C. Baker, A. Pradhan, L. Pakstis, D. J. Pochan and S. I. Shah, *J. Nanosci. Nanotechnol.*, 2005, **5**, 244–249.
- 20 V. K. Sharma, R. A. Yngard and Y. Lin, *Adv. Colloid Interface Sci.*, 2009, **145**, 83–96.
- 21 P. Huang, D. P. Yang, C. Zhang, J. Lin, M. He, L. Bao and D. Cui, *Nanoscale*, 2011, **3**, 3623–3626.
- 22 R. Lu, D. Yang, D. Cui, Z. Wang and L. Guo, *Int. J. Nanomed.*, 2012, **7**, 2101–2107.
- 23 K. Tseng, Y. Chen and J. Shyue, *J. Nanopart. Res.*, 2011, **13**, 1865–1872.
- 24 R. Khaydarov, R. Khaydarov, O. Gapurova, Y. Estrin and T. Scheper, *J. Nanopart. Res.*, 2009, **11**, 1193–1200.
- 25 G. Xi, J. Hui, Z. Zhang, S. Liu, X. Zhang, G. Teng, K. C. Chan, E. X. Wu, B. Nie, B. Shan, L. Li and G. P. Reynolds, *PLoS One*, 2011, **6**, e28686.
- 26 M. Garcia-Barros, F. Paris, C. Cordon-Cardo, D. Lyden, S. Rafii, A. Haimovitz-Friedman, Z. Fuks and R. Kolesnick, *Science*, 2003, **300**, 1155–1159.
- 27 J. H. Hendry, C. S. Potten and A. Merritt, *Radiat. Environ. Biophys.*, 1995, **34**, 59–62.
- 28 E. S. Redgate, M. Deutsch and S. S. Boggs, *Lab. Anim. Sci.*, 1991, **41**, 269–273.
- 29 B. Grobbs, P. P. De Deyn and H. Slegers, *Cell Tissue Res.*, 2002, **310**, 257–270.
- 30 K. Kalishwaralal, E. Banumathi, S. Ram Kumar Pandian, V. Deepak, J. Muniyandi, S. H. Eom and S. Gurunathan, *Colloids Surf., B*, 2009, **73**, 51–57.
- 31 S. Gurunathan, K. J. Lee, K. Kalishwaralal, S. Sheikpranbabu, R. Vaidyanathan and S. H. Eom, *Biomaterials*, 2009, **30**, 6341–6350.
- 32 S. Sheikpranbabu, K. Kalishwaralal, D. Venkataraman, S. H. Eom, J. Park and S. Gurunathan, *J. Nanobiotechnol.*, 2009, **7**, 8.
- 33 S. Sheikpranbabu, K. Kalishwaralal, K. J. Lee, R. Vaidyanathan, S. H. Eom and S. Gurunathan, *Biomaterials*, 2010, **31**, 2260–2271.
- 34 P. V. Asharani, M. P. Hande and S. Valiyaveetil, *BMC Cell Biol.*, 2009, **10**, 65.
- 35 M. I. Sriram, S. B. Kanth, K. Kalishwaralal and S. Gurunathan, *Int. J. Nanomed.*, 2010, **5**, 753–762.
- 36 D. De Stefano, R. Carnuccio and M. C. Maiuri, *J. Drug Delivery*, 2012, **2012**, 167896.
- 37 H. Y. Nam, S. M. Kwon, H. Chung, S. Y. Lee, S. H. Kwon, H. Jeon, Y. Kim, J. H. Park, J. Kim, S. Her, Y. K. Oh, I. C. Kwon, K. Kim and S. Y. Jeong, *J. Controlled Release*, 2009, **135**, 259–267.
- 38 J. S. Park, T. H. Han, K. Y. Lee, S. S. Han, J. J. Hwang, D. H. Moon, S. Y. Kim and Y. W. Cho, *J. Controlled Release*, 2006, **115**, 37–45.
- 39 Y. Zheng, D. J. Hunting, P. Ayotte and L. Sanche, *Radiat. Res.*, 2008, **169**, 19–27.

- 40 N. Bouzubar, K. J. Walker, K. Griffiths, I. O. Ellis, C. W. Elston, J. F. Robertson, R. W. Blamey and R. I. Nicholson, *Br. J. Cancer*, 1989, **59**, 943–947.
- 41 K. Maeda, Y. S. Chung, S. Takatsuka, Y. Ogawa, N. Onoda, T. Sawada, Y. Kato, A. Nitta, Y. Arimoto, Y. Kondo and M. Sowa, *Br. J. Cancer*, 1995, **72**, 319–323.
- 42 B. A. Rupnow and S. J. Knox, *Apoptosis*, 1999, **4**, 115–143.
- 43 D. Eriksson and T. Stigbrand, *Tumor Biol.*, 2010, **31**, 363–372.
- 44 K. C. Zimmermann, C. Bonzon and D. R. Green, *Pharmacol. Ther.*, 2001, **92**, 57–70.
- 45 P. Teixeira and S. Menezes, *Int. J. Radiat. Biol.*, 1996, **69**, 345–350.
- 46 A. H. Nias, *Int. J. Radiat. Biol. Relat. Stud. Phys., Chem. Med.*, 1985, **48**, 297–314.